Carcinogenesis vol.32 no.4 pp.597–604, 2011
doi:10.1093/carcin/bgq282
Advance Access publication December 24, 2010

Aberrant DNA hypermethylation patterns lead to transcriptional silencing of tumor suppressor genes in UVB-exposed skin and UVB-induced skin tumors of mice

Vijayalakshmi Nandakumar[1], Mudit Vaid[1], Trygve O.Tollefsbol[2] and Santosh K.Katiyar[1,3,*]

[1]Department ofDermatology, [2]Department of Biology, University of Alabama at Birmingham, 1670, University Boulevard, Volker Hall 557, AL 35294,USA and [3]Birmingham Veterans Affairs Medical Center, Birmingham, AL 35294, USA

*To whom correspondence should be addressed. Tel: +1 205 975 2608; Fax: +1 205 934 5745;
Email: skatiyar@uab.edu

Overexposure of the human skin to solar ultraviolet (UV) radiation is the major etiologic factor for development of skin cancers. Here, we report the results of epigenetic modifications in UV-exposed skin and skin tumors in a systematic manner. The skin and tumor samples were collected after chronic exposure of the skin of SKH-1 hairless mice to UVB radiation using a well-established photocarcinogenesis protocol. We found a distinct DNA hypermethylation pattern in the UVB-exposed epidermal skin and UVB-induced skin tumors that was associated with the elevated expression and activity of the DNA methyltransferases (Dnmt) 1, Dnmt3a and Dnmt3b. To explore the role of hypermethylation in skin photocarcinogenesis, we focused on the p*16*^{INK4a} and *RASSF1A* tumor suppressor genes, which are transcriptionally silenced on methylation. We established that the silencing of these genes in UVB-exposed epidermis and UVB-induced skin tumors is associated with a network of epigenetic modifications, including hypoacetylation of histone H3 and H4 and increased histone deacetylation, as well as recruitment of methyl-binding proteins, including MeCP2 and MBD1, to the methylated CpGs. Higher levels of DNA methylation and DNMT activity in human squamous cell carcinoma specimens than in normal human skin suggest that the data are relevant clinically. Our data indicate for the first time that UVB-induced DNA hypermethylation, enhanced Dnmt activity and histone modifications occur in UVB-exposed skin and UVB-induced skin tumors and suggest that these events are involved in the silencing of tumor suppressor genes and in skin tumor development.

Introduction

Ultraviolet (UV) radiation-induced epigenetic modifications in the skin and skin tumors have been reported and may contribute to the development of skin cancers, but the modifications and their effects have not yet been defined in a systematic study. DNA methylation at the 5′ cytosines, primarily at the CpG islands, affects gene expression in many biologic processes such as differentiation, genomic imprinting, DNA mutation and DNA repair (1–3). DNA methylation is the most characterized epigenetic mechanism that can be inherited without changing the DNA sequence (4). Global DNA hypomethylation and regional hypermethylation occur in tumorigenesis (5,6) and the importance of promoter hypermethylation as well as global hypomethylation in carcinogenesis has been discussed (7–10). It has been shown that both of these events can contribute to carcinogenesis through various mechanisms including silencing of tumor suppressor genes, upregulation of oncogenes and/or a reduction in genomic stability (11,12). It also has been reported that approximately half of the tumor suppressor genes that are inactivated in sporadic cancers are more often inactivated by epigenetic, than by genetic, mechanisms. Inactivation of genes with tumorsuppressor properties exclusively by epigenetic mechanisms has been shown in mouse models of human neoplasia (13,14). DNA hypermethylation is a major epigenetic mechanism in the silencing of the expression of tumor suppressor genes (7–9,15). DNA methylation is not only involved in the regulation of tumor suppressor genes in cancers but also in the regulation of genomic imprinting and X-chromosome inactivation (3,12). Hypermethylation of CpG dinucleotides in the 5′ regulatory region initiates the recruitment of methyl-CpG domain (MBD) containing proteins, such as MeCP2 or MBD1, that mediate the formation of a repressive chromatin (16,17). Although well studied, the various chromatin signatures and the distinctive features of each of these proteins vary in a tissue- and gene-specific manner (18), which is an area of research that requires more detailed investigation.

DNA methyltransferases (Dnmts) have been identified that initiate the methylation at position 5 of cytosines of CpG dinucleotides. Dnmt1 is the enzyme responsible for maintenance of mammalian DNA methylation during DNA replication using hemimethylated DNA, whereas Dnmt3a and Dnmt3b, which are encoded by different genes (19,20), are *de novo* methylases. *De novo* methylases can act as transcriptional repressors by using their ATRX domain to recruit HDAC1 (21,22). It has been observed that chronic inflammation markedly accelerates acquisition of DNA methylation changes (23,24). In basal and squamous cell carcinoma (SCC) lesions, aberrant promoter methylation has been reported, with a high frequency of methylation of several tumor suppressor genes known to be associated with skin cancers, such as CDH1, CDH3, LAMA3, LAMC2 and RASSF1A as well as others (25). We examined the effects of chronic UVB exposure on epigenetic modifications in the skin of mice as well as in the UVB-induced skin tumors and demonstrate hypermethylation of DNA accompanied by H3 and H4 hypoacetylation in the mouse skin after chronic exposure to UVB radiation. We also demonstrate that epigenetic mechanisms are associated with the silencing of the tumor suppressor genes, p*16*^{INK4a} and *RASSF1A*, which are candidate tumor suppressor genes associated with the development of skin cancer on chronic UVB exposure of the mouse skin.

Abbreviations: Dnmt, DNA methyltransferase; 5-mC, 5-methylcytosine; mRNA, messenger RNA; PCR, polymerase chain reaction; SCC, squamous cell carcinoma; UV, ultraviolet.

Materials and methods

Animals

The six-to-seven-week-old female SKH-1 hairless mice used in this study were obtained from Charles River Laboratories (Wilmington, MA). All mice were housed in the Animal Resource Facility of the University of Alabama at Birmingham under the following conditions: 12 h dark/12 h light cycle, 24 ± 2°C temperature and 50 ± 10% relative humidity. The mice were fed a standard Purina Chow diet and water *ad libitum*. The animal protocol used in this study was approved by the Institutional Animal Care and Use Committee of the University of Alabama at Birmingham.

Antibodies and reagents

Antibodies were purchased as follows: 5-methylcytosine (5-mC) from Calbiochem, EMD Biosciences (New Jersey, NJ), Dnmt1, Dnmt3a and Dnmt3b from Imgenec Corporation (San Diego, CA); HDAC1 from Upstate Antibodies (NY) and acetyl histone H4, acetyl histone H3, MBD1 and MeCP2 from Abcam Antibodies (Cambridge, MA). RNA and DNA isolation kits were purchased from Invitrogen (Carlsbad, CA). The Methylamp™ Global DNA Methylation Quantification Kit and the EpiQuik DNA Methyltransferase Activity Assay Kit were purchased from Epigentek (New York, NY). Standardized real-time polymerase chain reaction (PCR) primers for Dnmt1, Dnmt3a, Dnmt3b, p*16*^{INK4a} and *RASSF1A* were obtained from SuperArray Biosciences Corporation (Fredrick, MD). MOD50 Bisulfite Modification Kit and all other chemicals of analytical grade were purchased from Sigma Aldrich Chemical Co. (St. Louis, MO)

UVB irradiation and photocarcinogenesis protocol

The dorsal area of the SKH-1 hairless mice was exposed to UV radiation from a band of four UV lamps (Daavlin, UVA/UVB Research Irradiation Unit,

Bryan, OH) equipped with an electronic controller to regulate UV dosage, as described earlier (26). At least 1 week after their arrival in the animal facility, the mice were divided into two experimental groups with 20 mice in each group. Mice in Group 1 were not subjected to UVB irradiation and this group served as a control, whereas mice in Group 2 were subjected to UVB irradiation (180 mJ/cm^2) three times a week for a total of 24 weeks. At the termination of the experiment, mice were killed and tumor and tumor un involved skin samples were collected for the analysis. The skin and skin tumor samples used in this study were obtained from our previous study (27), as detailed above. In a separate set of experiment, mice were exposed to UVB (180 mJ/cm^2) radiation three times per week. Mice were killed at four different time points after UVB exposure, such as 4, 8, 12 and 24 weeks, and skin samples were collected for the analyses of epigenetic biomarkers.

Procurement of human skin tumor samples

Thirteen samples of human SCCs (eight male, five female; age, 49–79 years) were obtained from the Tumor Tissue Procurement Facility tissue bank of the Comprehensive Cancer Center of the University of Alabama at Birmingham. Approval from the Institutional Review Board was obtained for the procurement of these specimens and their use in this study.

Immunohistochemical detection of DNA methylation patterns

Paraffin-embedded skin and tumor sections (6 μm thick) were deparaffinized and rehydrated in a graded series of alcohols. Following rehydration, an antigen retrieval process was carried out as detailed earlier (27). The sections were then treated with 3% H_2O_2 for 20 min to quench endogenous peroxidase. Sections were incubated with preimmune goat serum (3%) for 30 min to suppress non-specific binding. The sections were incubated subsequently with antibody specific for 5-mC (10 μg/ml; IgG1 isotype) for 90 min. After washing the slides, bound anti-5-mC antibody was detected by incubation with biotinylated goat anti-mouse IgG1 followed by peroxidase-labeled streptavidin. Sections were then incubated with diaminobenzidine plus peroxidase substrate and counterstained with hematoxylin.

Dot blot analysis of cyclobutane pyrimidine dimers

Genomic DNA from epidermal skin and tumor samples was isolated following the standard procedures and dot blot analysis was performed as detailed previously (26). Briefly, genomic DNA (500 ng) was transferred to a positively charged nitrocellulose membrane by vacuum dot blotting (Bio-Dot Apparatus; Bio-Rad, Hercules, CA) and fixed by baking the membrane for 30 min at 80°C. After blocking the non-specific binding sites in blocking buffer, the membrane was incubated with the antibodies specific to cyclobutane pyrimidine dimers for 1 h at room temperature. After washing, the membrane was incubated with horseradish preoxidase-conjugated secondary antibody. The circular bands of cyclobutane pyrimidine dimers were detected by chemiluminescence using ECL detection system.

Immunohistochemical detection of Dnmts

Paraffin-embedded skin and tumor sections (6 μm thick) were deparaffinized, subjected to the antigen retrieval process (27), then permeabilized in 0.1% Triton-X 100 (Sigma Chemical Co.) for 30 min. After quenching the endogenous peroxidase in H_2O_2 and suppressing the non-specific staining with goat serum, the sections were incubated with antibodies specific for Dnmt1, Dnmt3a or Dnmt3b overnight at 4°C. Bound anti-Dnmts antibody was detected by incubation with biotinylated goat anti-mouse IgG1 followed by peroxidase-labeled streptavidin. Sections were then incubated with diaminobenzidine and counterstained with hematoxylin.

Assay for global DNA methylation

The total genomic DNA was extracted from the mouse epidermis or tumor samples using the Qiagen amp^R DNA Mini Kit (Qiagen Sciences, Valencia, CA) following the manufacturer's instructions. The Global DNA methylation levels were determined using the Methylamp^{TM} Global DNA Methylation Quantification Kit according to the manufacturer's instructions. This analysis provides the levels of global DNA methylation and is not specific to any particular gene. The data are presented in terms of percent of control (non-UVB-exposed epidermal skin).

Preparation of tumor and skin lysates for western blotting

Epidermal or tumor lysates for western blot analysis were prepared as described previously (28,29). The tissue samples were pooled from at least three mice in each group, and three sets of pooled samples from each treatment group were used for western blot analysis, n = 9–10. Briefly, proteins (30–50 μg) were resolved on 10% Tris–glycine gel and transferred onto nitrocellulose membranes, which were incubated in blocking buffer and then incubated with the primary antibodies, i.e. HDAC1, acetyl histone H4 (Lys 16), acetyl histone H3 (K9), MBD1 or MeCP2, in blocking buffer overnight at 4°C. The membranes were then washed and incubated with the appropriate secondary antibodies conjugated with horseradish peroxidase. Protein bands were visualized using enhanced chemiluminescence reagents (Amersham Life Science, Piscataway, NJ). To verify equal protein loading, the blots were stripped and reprobed for β-actin. The density of each band in an immunoblot and dot blot was determined using the Scion Image Program (National Institutes of Health, Bethesda, MD). The relative numerical values are shown under each immunoblot. The values for the control group (non-UVB-exposed) were assigned the value '1' (arbitrary unit) and comparison was then made with densitometry values of other treatment groups.

Quantitative analysis of Dnmts using real-time PCR

Total RNA was extracted from the tissue samples using Trizol Reagent Kit (Invitrogen). Complementary DNA was synthesized using 1 μg RNA through the reverse transcription reaction (iScript cDNA Synthesis Kit; Bio-Rad). Using SYBR Green/Fluorescein PCR Master Mix, complementary DNA was amplified using real-time PCR with a Bio-Rad MyiQ thermocycler and SYBR Green detection system (Bio-Rad). Samples were run in duplicate to ensure amplification integrity. Manufacturer-supplied standardized primer pairs were used to measure the following: Dnmt1, Dnmt3a, Dnmt3b, p*16^{INK4a}* and *RASSF1A*. The standard PCR conditions were: 95°C for 15 min and then 40 cycles at 95°C for 30 s, 55°C for 30 s and 72°C for 30 s, as recommended (SuperArray Biosciences Corporation). The messenger RNA (mRNA) expression levels of genes were normalized to the expression level of the β-actin mRNA in each sample using the cycle threshold (C_t) method and using the $2^{-\Delta Ct}$ formula.

Assay for Dnmts activity

The tissue samples were pooled from at least three mice in each group, and five sets of pooled samples from each treatment group were used to prepare nuclear extracts. Nuclear extracts were prepared using EpiQuik^{TM} Nuclear Extraction Kit I (Epigentek), and Dnmt activity was determined using the EpiQuik DNA Methyltransferase Activity Assay Kit (Epigentek) according to the manufacturer's instructions. This analysis provides the levels of overall Dnmt activity and is not specific to any particular gene or not specific to any particular Dnmt (such as Dnmt1, Dnmt3a or Dnmt3b), and the data are presented in terms of percent of control (non-UVB-exposed epidermal skin).

Chromatin immunoprecipitation assays

To assess the levels of histone acetylation and the methyl-binding proteins in the p*16^{INK4a}* and *RASSF1A* promoter regions, the EpiQuik^{TM} Tissue Chromatin Immunoprecipitation Kit (Epigentek) was used. Briefly, the number of strip wells required for the assay was incubated with antibodies specific for HDAC1, acetyl histone H4, acetyl histone H3, MBD1 or MeCP2. A no-antibody negative control well was used for each of the antibodies and incubated for 2 h at 4°C. UV-exposed or non-UV-exposed tissue samples (≈40 mg) were cross-linked with 1% formaldehyde and disaggregated in a Teflon homogenizer using homogenizing buffer supplied with the kit. Cross-linked DNA was sheared using ultrasonic homogenizer (Model 150 V/T; Biologics, Manassas, VA) to approximately 200–1000 bp in length and centrifuged. The supernatant was added to the antibody-coated wells and incubated at room temperature on a shaker. The cross-linked DNA, including the inputs, was reversed by incubation at 65°C and the immunoprecipitated DNA was then captured, purified and eluted using the specifically designed Fast-Spin Columns. The purified DNA was amplified by standard PCR for p*16^{INK4a} region*, amplifying fragment spanning from 88928422 to 88928811 (negative strand; Chr 4; UCSC genome browser) using 5′-CAGATTGCCCTCCGATGACTTC-3′and 5′-TGGACCCGCACAGCAAAGAAGT-3′ and for *RASSF1A region*, amplifying a fragment of the promoter spanning from 107456306 to 107456495 (positive strand; Chr 9; UCSC genome browser) with the primers, 5′-GTGTCCAGAGGTGCCTAACC-3′ and 5′-AACGGTAATGGCAGGTGAAC-3′. PCR was performed under the following conditions: 95°C for 5 min; 94°C for 30 s, 60°C for 1 min, 72°C for 1 min—40 cycles; 72°C for 5 min for p*16^{INK4a}* region and 95°C for 5 min, 95°C for 30 s, 56°C for 1 min, 72°C for 1 min—35 cycles; 72°C for 5 min for the *RASSF1A* region.

Methylation-specific PCR, bisulfite conversion

The DNA from skin and tumor samples was extracted using the Qiagen amp^R DNA Kit. One microgram of genomic DNA was treated with bisulfite and incubated at 99°C for 6 min, then 65°C for 90 min followed by post purification steps as per the manufacturer's instruction in the MOD50 Bisulfite Modification Kit (Sigma Aldrich, St. Louis, MO). The bisulfite-converted samples were amplified using primers specific for the methylated and the unmethylated regions of p*16^{INK4a}* and *RASSF1A* (30,31), as detailed below:

p*16^{INK4a}*, methylated: forward CGATTGGGCGGGTATTGAATTTTCGC and reverse CACGTCATACACAC GACCCTAAACCG and unmethylated: forward GTGATTGGGTGGGTATTGAATTTTTGTG and reverse CACACATCATACACACACAACCCTAAACA. *RASSF1A*, methylated: forward

TTTTGCGGTTTCGTT CGTTC and reverse CCCGAAACGTACTACTA-TAAC and unmethylated: forward GGTGTTGAAGTTGTGGTTTG and reverse TATTATACCCAAAACAATACAC. Conditions for $p16^{INK4a}$: 95°C for 10 min, 94°C for 30 s, 64–66°C for 1 min, 72°C for 1 min– for 40 cycles, 72°C for 8 min. Conditions for *RASSF1A*: 95°C for 5 min, 95°C for 30 s, 53–55°C for 1 min, 72°C for 1 min for 38 cycles, 72°C for 8 min. The PCR products were run on 1.5% agarose gels and visualized using a trans-UV illuminated Gel-doc Machine (Bio-Rad).

Statistical analysis

The results of the real-time PCR are expressed as the means ± standard deviations. The other data are expressed as percentages with the basal levels in skin samples that were not exposed to UVB radiation taken as 100% for the Dnmt activity and global DNA methylation levels. Statistical analysis was carried out using one-way analysis of variance between the UV-exposed skin or skin tumors versus non-UVB-exposed skin samples followed by *post hoc* tests. The difference between the experimental groups was considered significant if $P < 0.05$.

Results

UVB irradiation of the skin stimulates DNA methylation

As UVB-induced skin tumors primarily arise from the epidermis of the skin, we have used epidermis of the whole skin for all the analytical purposes. Therefore, the use of word skin means epidermis of the skin for epigenetic modifications. As chronic UV irradiation results in skin tumor development in mice, we sought to determine whether there is a disruption of the DNA methylation patterns in the UVB-exposed skin of the groups of mice that had been exposed to UVB radiation for 24 weeks (UVB-exposed skin) and the UVB-induced tumors as compared with the skin of the groups of mice that were not exposed to UVB radiation (non-UVB-exposed skin). Immunostaining suggested greater DNA methylation in the UVB-exposed epidermal skin and the UVB-induced skin tumors than in the non-UVB-exposed epidermis (Figure 1A). This was further confirmed by dot blot analysis with the relative density of each dot blot (Figure 1B). Quantitative analysis of the global DNA methylation levels showed that the DNA methylation in the UVB-exposed epidermal skin was >100% ($P < 0.001$) higher than in the non-UVB-exposed epidermis and that the DNA methylation in the UVB-induced skin tumors was ~3-fold higher ($P < 0.001$) than in the non-UVB-exposed skin (Figure 1C). These data show that the DNA in mouse skin acquires aberrant methylation on chronic UVB exposure. Analysis of the kinetics of global DNA methylation in the UVB-exposed skin revealed that the levels of global DNA methylation increased (60–140%, $P < 0.01$–0.001) as the length of time of exposure to the UVB radiation increased (Figure 1D).

UVB irradiation stimulates Dnmts, mRNA expression and activity

As Dnmts play a crucial role in DNA methylation, we determined the expression profiles of Dnmt1, Dnmt3a and Dnmt3b. Immunostaining of the skin revealed that the Dnmts are expressed in the non-UVB-exposed epidermis; however, the expression of Dnmt1, Dnmt3a and Dnmt3b was higher in the UVB-exposed epidermis than the non-UVB-exposed epidermis of the skin (Figure 2A). Additionally, the expressions of Dnmt3a and Dnmt3b were also found to be expanded in other cells in UVB-exposed epidermis of the skin than normal epidermis of the skin. Immunostaining of the UVB-induced tumors indicated that the intensity of Dnmt1, Dnmt3a and Dnmt3b was greater in the skin tumors than the non-UVB-exposed skin, with the intensity of staining of Dnmt1 in the tumors being relatively greater than the intensity of staining of Dnmt3a and Dnmt3b. These results were consistent with the quantitative analysis of the mRNA expression of the Dnmts using real-time PCR. The mRNA levels of Dnmt1, Dnmt3a and Dnmt3b were significantly higher ($P < 0.01$ to $P < 0.001$) in the UVB-exposed skin and the UVB-induced skin tumors as compared with the non-UVB-exposed epidermis of the skin (Figure 2B). The Dnmt activity in the UVB-exposed epidermis and UVB-induced tumors was >2–- to 3-fold higher than the activity in non-UV-exposed epidermis (Figure 2C). There was a significant increase in Dnmt activity (70%, $P < 0.01$) after 4 weeks of UVB irradiation, followed by a sustained gradual increase through week 24 of UVB exposure.

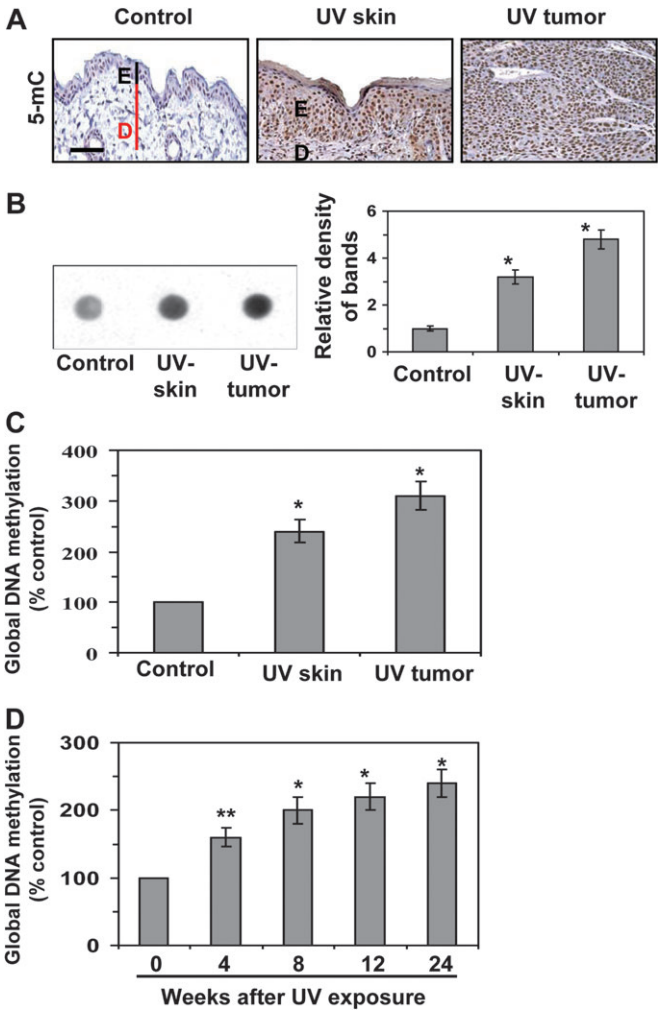

Fig. 1. UVB irradiation stimulates DNA methylation in the skin. DNA methylation was assessed in UVB-exposed epidermal skin, skin tumors and non-UVB-exposed epidermis of the skin from SKH-1 hairless mice at the termination of a 24 weeks photocarcinogenesis protocol. (**A**) Immunohistochemical detection of DNA methylation using a 5-mC-specific antibody and counterstaining with hematoxylin and eosin. Positive staining is dark brown. Bar, 50 μm. (**B**) Dot blot analysis of levels of 5-mC in DNA extracted from the epidermis or whole tumors; $n = 10$. Data are also presented in terms of relative density of dot blots in different treatment groups. (**C**) Quantitative analysis of global DNA methylation, $n = 10$. (**D**) Global DNA methylation levels in the epidermal skin at different time points after UVB exposure of the skin; $n = 10$. In (C and D), data are presented in terms of percentage versus the results using epidermis from non-UVB-exposed control mice, which was assigned a value of 100%, and as means ± SD; $n = 5$. Significant difference versus unexposed skin, $^{**}P < 0.01$; $^{*}P < 0.001$; E, epidermis; D, dermis.

Distribution patterns of Dnmt1-, Dnmt3a- and Dnmt3b-positive cells in UVB-irradiated skin/epidermis

We observed differential expression of the Dnmts in the epidermis. As can be seen in Figure 2A, in the UVB-exposed skin, the Dnmt1-positive cells with enhanced staining were found throughout the epidermis. In contrast, the Dnmt3a- and Dnmt3b-positive cells with enhanced staining were localized primarily in the basal cell layer of the epidermis. As the basal layer of the epidermis is a proliferating cell layer, these observations suggest that Dnmt3a and Dnmt3b may be associated with the increased cellular proliferation that is typical of chronic UVB exposure.

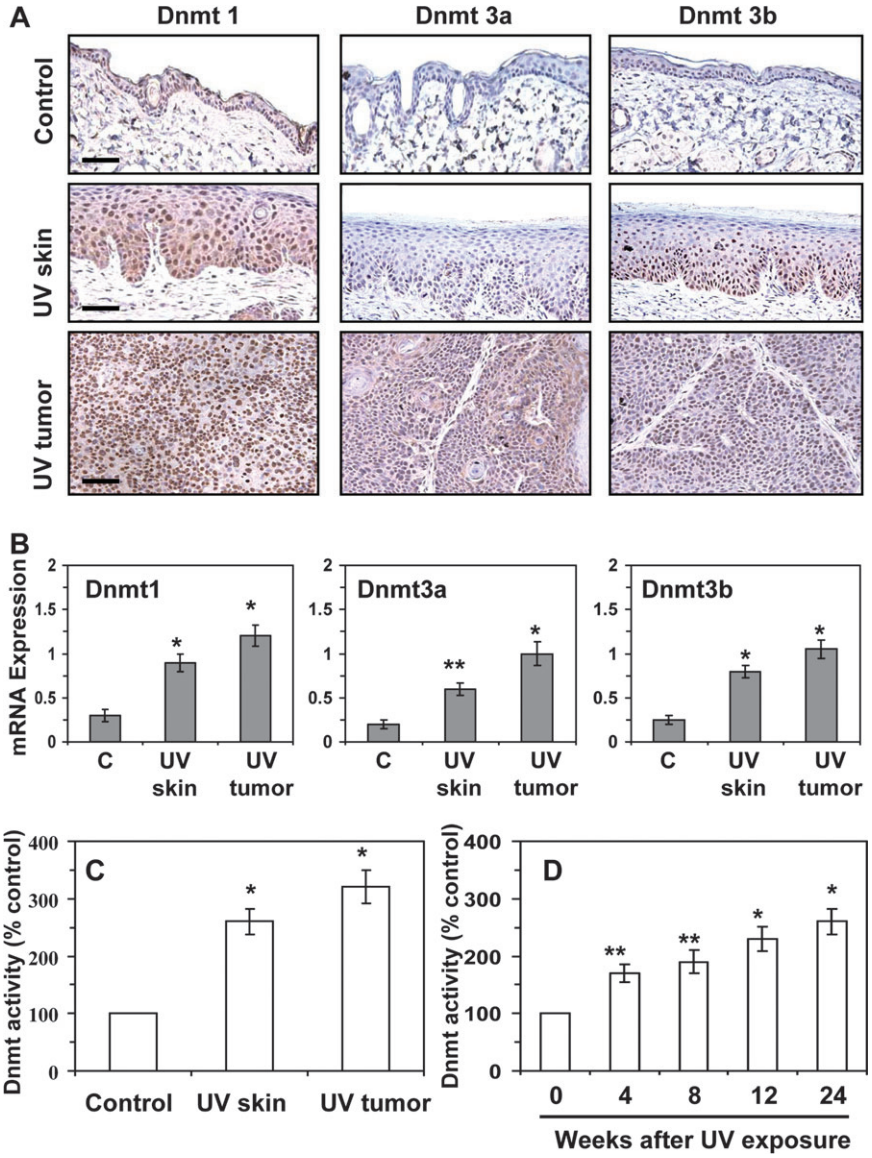

Fig. 2. UVB irradiation enhances the levels and activity of Dnmts in the skin. (**A**) Immunohistochemical detection of Dnmt1, Dnmt3a and Dnmt3b; bar, 50 μm. (**B**) Real-time PCR analysis of mRNA levels of Dnmt1, Dnmt 3a and Dnmt 3b in epidermal tissues and tumors. The results are presented as the expression of the individual mRNA with normalization to β-actin, and as mean values ± SD; $n = 6$. (**C**) Dnmt activity in nuclear extracts was determined using the DNA Methyltransferase Activity Assay Kit. (**D**) Dnmt activity in the epidermal skin at different time points after UVB exposure of the skin. In (C and D), data are presented in terms of percentage versus the results using non-UVB-exposed mouse epidermis, which was assigned a value of 100%, and as means ± SD; $n = 6$. Significant difference versus non-UVB-exposed control skin, $^{**}P < 0.01$, $^{*}P < 0.001$.

Analysis of the chromatin remodeling factors associated with DNA hypermethylation

DNA hypermethylation leading to the recruitment of the methyl-binding domain (MBD) family of proteins that mediate silencing of genes via formation of a repressive chromatin environment is a common phenomenon in many cancers (32,33). We therefore subjected skin and tumor lysates to western blot analyses using antibodies specific for HDAC1, acetylated-H3, acetylated-H4, MBD1 and MeCP2. The levels of HDAC1 were higher in the UVB-exposed skin and UVB-induced skin tumors as compared with non-UVB-exposed skin, whereas the levels of acetylated-H3 and -H4 were lower in the UVB-exposed skin, indicating a global increase in the histone deacetylation and a decrease in the histone acetylation on UVB-induced DNA hypermethylation (Figure 3). MeCP2 and MBD1 showed an overall greater recruitment to the methylated CpGs on chronic UV exposure of the mouse skin as well as in skin tumors.

Gene-specific epigenetic modifications associated with UVB-induced DNA methylation

To determine whether the UVB-induced epigenetic modifications in the mouse skin and tumors are gene specific, we chose to analyse the promoter regions of p*16*^{INK4a} and *RASSFIA* as several reports have identified p*16*^{INK4a} and *RASSFIA* as the best-characterized tumor suppressor genes in both malignant and non-malignant skin lesions (25,34–36). We analyzed the methylation status of p*16*^{INK4a} and *RASSF1A* using methylation-specific PCR with primers specific for methylated and unmethylated sequences. The PCR amplifications were carried out after bisulphite conversion. Our results clearly show higher levels of DNA methylation in the UVB-exposed skin and UVB-induced tumors as compared with the non-UVB-exposed skin (Figure 4A). This effect was observed for both the p*16*^{INK4a} and *RASSF1A* genes and was accompanied by a simultaneous reduction in the levels of unmethylated DNA of the p*16*^{INK4a} and *RASSF1A* genes. DNA hypermethylation of p*16*^{INK4a} and *RASSF1A* has been

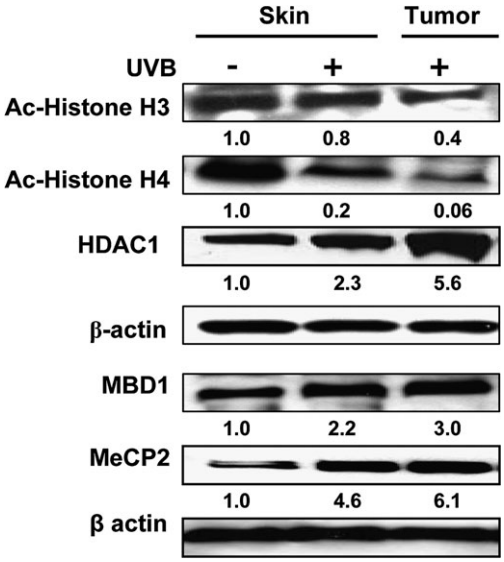

Fig. 3. Expression of the various chromatin remodeling and methyl-binding proteins associated with the hypermethylated DNA of UVB-exposed mouse skin and UVB-induced tumors obtained after 24 weeks of the photocarcinogenesis protocol. The levels of Ac-hisone H3, Ac-histone H4, HDAC1, MBD1 and MeCP2 were determined in lysates using western blotting. Skin samples from non-UVB-irradiated mice were used as controls. A representative blot is shown from three independent experiments with identical results and the relative density of each band (arbitrary) is shown under the immunoblot in terms of fold change compared with normal non-UVB-exposed epidermal skin.

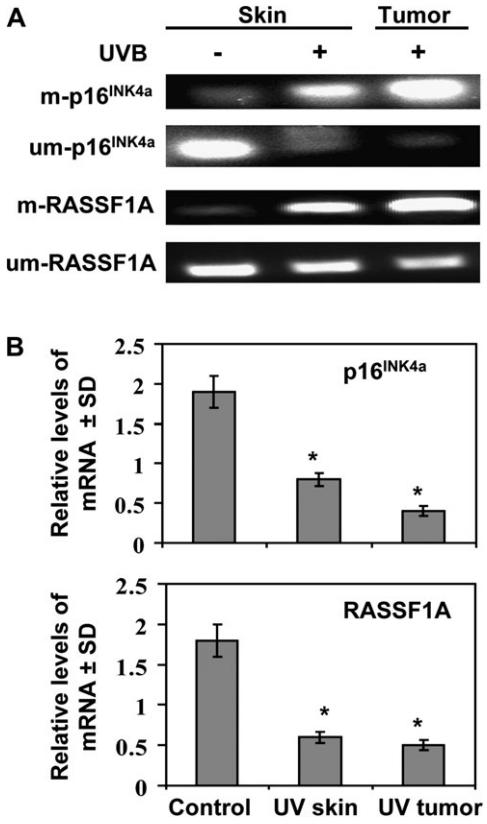

Fig. 4. Analyses of the methylated and unmethylated status of DNA and the mRNA expression of the p*16*^{INK4a} and *RASSF1A* genes in UVB-exposed epidermal skin and UVB-induced tumors obtained after 24 weeks of the photocarcinogenesis protocol. (**A**) DNA was extracted and processed for sodium bisulfite conversion and the levels of methylated and unmethylated DNA were determined using real-time PCR. (**B**) Total RNA was isolated and the mRNA transcripts of the p*16*^{INK4a} and *RASSF1A* genes quantified using the real-time PCR SYBR Green system. Data are presented as a relative change in mRNA transcript levels in UVB-exposed epidermal skin and UVB-induced tumors as compared with the levels in the skin of unexposed control mice and are expressed as mean values ± SD; $n = 6$. Significant difference versus control skin, $^{*}P < 0.001$.

shown to be associated with downregulation of their mRNA levels (18,37,38). Analysis of the p*16*^{INK4a} and *RASSF1A* mRNA levels by real-time PCR showed significant lower ($P < 0.001$) mRNA levels of both p*16*^{INK4a} and *RASSF1A* genes in the UVB-exposed skin and UVB-induced skin tumors as compared with non-UVB-exposed skin (Figure 4B). Thus, these data show that downregulation of these tumor suppressor genes associated with DNA hypermethylation and that is associated with chronic UVB exposure of the mouse skin.

Modifications in histones and methyl-binding proteins in skin are associated with the DNA hypermethylation on chronic UVB exposure

We further determined if the silencing of the hypermethylated tumor suppressor genes is associated with the acetylation and deacetylation of the histones in the chromatin assembly and if the methyl-binding proteins also contribute to the transcriptional downregulation of these tumor suppressor genes. To accomplish this, we carried out a chromatin immunoprecipitation analysis of the p*16*^{INK4a} and *RASSF1A* promoter regions using antibodies specific for HDAC1, acetylated-H3, acetylated-H4, MeCP2 and MBD1 (Figure 5A and B) and UVB-exposed epidermis of the skin and non-UVB-exposed epidermal tissue samples. The chromatin immunoprecipitation analysis data indicated an increase in MeCP2 and HDAC1 associated with p*16*^{INK4a} and in MeCP2, MBD1 and HDAC1 associated with *RASF1A*. The input DNA and the immunoprecipitated DNA were also amplified by primers specific for the p*16*^{INK4a} and *RASSF1A* regions using quantitative real-time PCR with normalization of the data to the input samples. The results showed a significant increase in the associated HDAC1 (60%, $P < 0.01$) and MeCP2 (83%, $P < 0.001$) and a significant decrease in acetylated-H4 (75%, $P < 0.001$) in the p*16*^{INK4a} promoter region (Figure 5C). Almost similar observations were found in the RASSF1A promoter region (Figure 5D). These results demonstrate the occurrence of histone hypoacetylation with the recruitment of the HDACs to the hypermethylated CpGs, which can bind to them either directly or through the methyl-binding proteins on chronic UVB exposure; however, our data do not exclude the possibility of involvement of other chromatin remodelers in this transcription silencing process.

DNA hypermethylation patterns and enhanced DNMT activity in human SCC

Immunohistochemical examination of the epigenetic modifications in human SCC samples revealed that the numbers of 5-mC-positive cells were markedly higher in human SCC samples obtained from 13 of 13 different patients as compared with non-SCC-involved human skin samples. A representative example is shown in Figure 6A, in which the 5-mC-positive cells that are dark brown in color, are distributed throughout the epidermis as well as the inner or deeper parts of the SCCs. The levels of global DNA methylation in the human SCCs were >3-fold higher ($P < 0.001$) as compared with the non-SCC-involved skin samples (Figure 6B), and the levels of DNMT activity in human SCCs were >4-fold higher ($P < 0.001$) as compared with non-SCC-involved skin samples (Figure 6C).

Discussion

The transition from a normal cell to a neoplastic cell is a complex process and involves both genetic and epigenetic changes (39,40), with the process of carcinogenesis beginning when the DNA is damaged (41). It is thought that the major mechanism by which UV

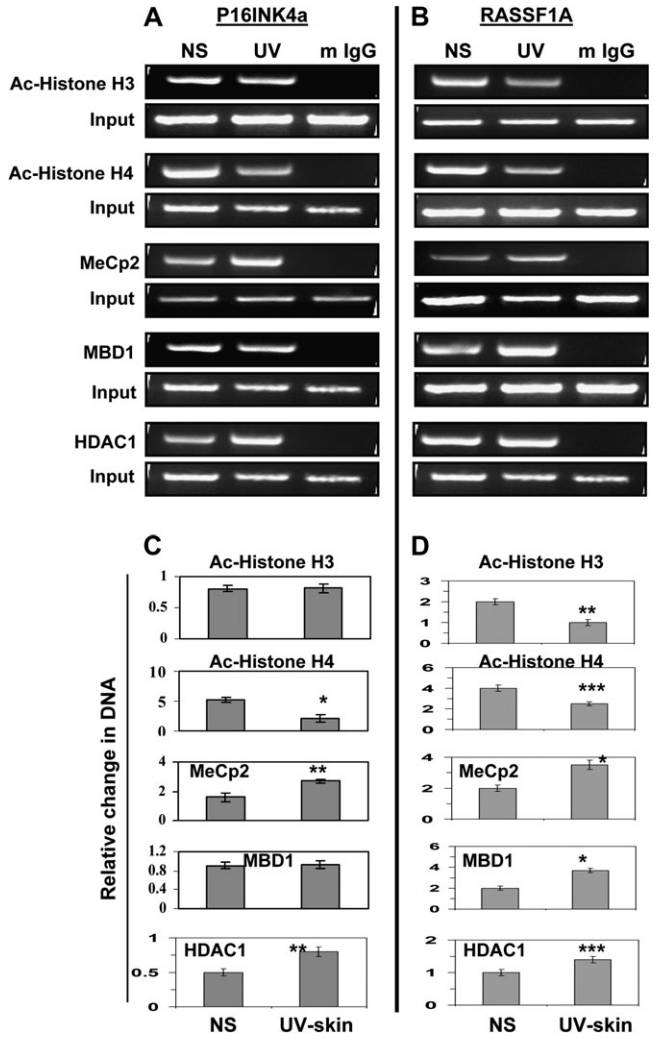

Fig. 5. Modifications in histones and methyl-binding proteins are associated with the DNA hypermethylation of the p*16*^{INK4a} and *RASSF1A* promoters in UVB-exposed epidermal skin after 24 weeks. (**A**) Chip analyses of Ac-histone H3, Ac-histone H4, MeCp2, MBD1 and HDAC1 in the p*16*^{INK4a} and (**B**) *RASSF1A* promoter regions. The panels show the PCR amplification product of the ChIP-purified DNA using the specific antibodies. Samples incubated with mouse IgG served as negative controls. (**C** and **D**) Quantification by real-time PCR using the same experimental procedures, antibodies and primers. Data were normalized to input samples and are presented as relative change in DNA and expressed in terms of mean values ± SD ($n = 3$, epidermal skin or tumor samples were used from three different mice per group). Significant difference versus non-UVB-exposed epidermal skin (normal skin) samples, $^{***}P < 0.05$, $^{**}P < 0.01$, $^{*}P < 0.001$.

radiation induces skin tumor development is via mutations of the p53 gene. The mutations are predominantly the UV signature mutation, i.e. a C→T transitions at dipyrimidine sites, which result from UV radiation-induced cyclobutane pyrimidine dimer formation (42). Notably, methylation of cytosine has been shown to enhance the pyrimidine dimer formation resulting from exposure of cells to solar UV radiation by 5-– to 15-fold due to the higher energy absorption of the 5-mC as compared with the cytosine in the DNA (42). Many of the signature mutations occur at CpG sites (42); thus, the presence of 5-mC in mammalian DNA adds to the UVB-associated mutational burden through several different mechanisms (2,4,6).

The major goal of this study was to systematically characterize the effect of UV radiation on the skin and skin tumors for epigenetic modifications, specifically DNA methylation and histone modifications. Our systematic analysis of UV-exposed skin and tumor samples indicates that UV exposure induces a DNA hypermethylation pattern in the epidermis of the skin and skin tumors of mice. Moreover, the DNA hypermethylation was consistent with the finding of enhanced levels of Dnmts in the UV-exposed mouse skin and tumors. Intriguingly, the different distribution patterns of the Dnmts within the UVB-exposed skin and the preferential distribution of the intensely staining Dnmt3a and Dnmt3b cells in the basal layer of the UVB-exposed skin suggests that the *de novo* synthesis of Dnmt3a and Dnmt3b may contribute to a major chromatin mark for cellular proliferation on chronic UVB exposure of the skin and within skin tumors. The findings of our study indicate that the increase in the levels of global DNA methylation and the levels of Dnmt activity occur relatively quickly in UV-exposed skin and prior to the onset of recognizable preneoplastic changes or the appearance of tumors. It has been shown that UV radiation induces p53 mutations and methylation in keratinocytes at a relatively early age in chronically sun-exposed areas of human skin (43). Mittal *et al.* (39) have reported finding DNA hypomethylation in sporadic patches; however, DNA hypermethylation is predominant over the sun-exposed skin and in skin tumors. The DNA hypomethylation pattern was not observed in skin tumors of mice in this study. Grönniger *et al.* (44) analyzed human skin samples exposed to chronic UV exposure for distinct epigenetic changes. This investigation identifies that aging and sun exposure are associated with comparably small, but significant changes in the DNA hypermethylation were found in aged samples than young samples.

Previous studies have shown an association between DNA hypermethylation and histone hypoacetylation with downregulation of the tumor suppressor genes (45,46). We found hypoacetylation of H3 and H4 histones in the transcriptionally silenced p*16*^{INK4a} and *RASSF1A* regions on UVB exposure. These 'hot spots' were selected based on the functional analysis reports, which indicated that the increased density of the promoter methylation of the p*16*^{INK4a} and *RASSF1A* was associated with altered chromatin rearrangements, marked by a depletion of acetylated histones H3 and H4 (30–32,35). We also found an increase in the recruitment of MeCP2 and MBD1 to the p*16*^{INK4a} and *RASSF1A* methylated heterochromatin on chronic UV exposure of the skin. These data suggest the involvement of MeCP2 and MBD1 in the chromatin remodeling and transcriptional silencing of the tumor suppressor genes p*16*^{INK4a} and *RASSF1A* on chronic UV exposure. It has been shown that generation of reactive oxygen species also caused hypermethylation of tumor suppressor genes, such as p16^{INK4a}. These studies implicated Akt, reactive oxygen-nuclear factor-kappaB association with loss of p^{16INK4a} to be important in melanoma growth as a solid tumor (47). Arbiser *et al.*. (48) also analyzed SCC from patients with recessive dystrophic epidermolysis bullosa and found the loss of p16^{INK4a} through hypermethylation and mutations in the p53 tumor suppressor genes. These studies demonstrate that alterations in both p53 and p16^{INK4a} can contribute to recessive dystrophic epidermolysis bullosa associated SCC.

Our data suggest a strong link between DNA methylation and histone acetylation on chronic exposure of the skin to UV irradiation; however, to fully understand the epigenetic pathways that are triggered by chronic UV exposure and their roles in the development of skin cancer, further studies of other tumor suppressor genes, oncogenes and other chromatin remodeling factors are needed. In this report, we demonstrate for the first time that chronic exposure of the mouse skin to UV radiation stimulates the expression and activity of Dnmts that may lead to the aberrant hypermethylation of DNA. This, in turn, stimulates DNA methylation-associated epigenetic mechanisms, such as the recruitment of MBDs and histone hypoacetylation. Collectively, these events are associated with the downregulation of tumor suppressor genes, most probably through the formation of closed chromatin structure. Similar findings, including DNA hypermethylation, global DNA methylation and increased DNMT activity in human SCC support the clinical significance of our findings generated using the mouse model and suggest that these epigenetic modulations in skin contribute to the tumor development in UV-exposed skin. Since epigenetic modifications are reversible, targeting of these events may lead to the development of novel therapeutic strategies for the prevention of skin cancers in humans. Such

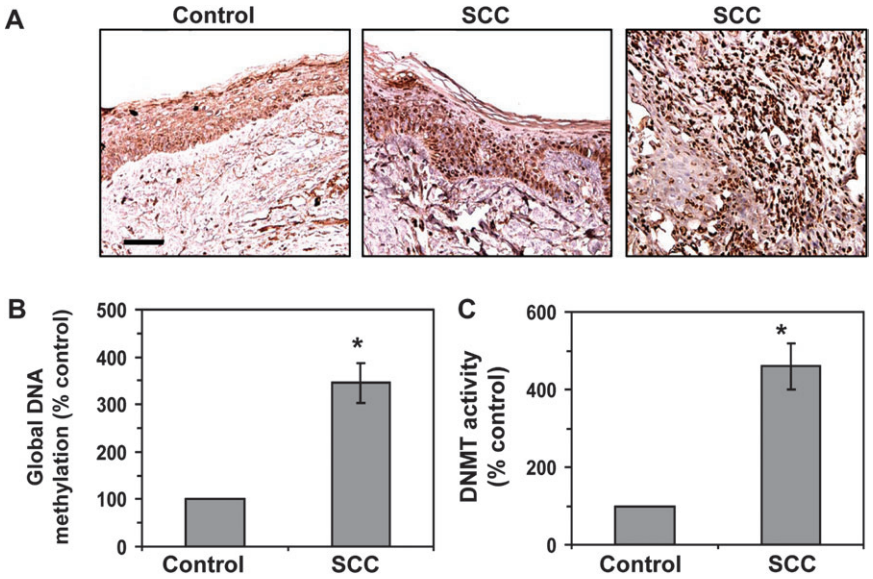

Fig. 6. DNA hypermethylation and enhanced levels of DNMT activity in human SCC tumor samples. (**A**) Immunohistochemical detection of DNA methylation-positive cells using 5-mC-specific antibody in frozen sections (5 μm thick) of SCC tumors and SCC-uninvolved skin (control); bar, 50 μm. The sections were counterstained with hematoxylin and eosin. Positive staining is dark brown. Representative photomicrographs are shown. Similar results were obtained in samples from 13 different patients with SCC. (**B**) Quantitative analysis of global DNA methylation using Global DNA Methylation Quantification Kit to analyse DNA samples from SCC tumors and SCC-uninvolved skin. (**C**) DNMT activity in nuclear extracts of SCC-uninvolved skin and SCC tumor samples as determined using the EpiQuik™ DNA Methyltransferase Activity Assay Kit. Data are presented as the percent of the value obtained for the SCC-uninvolved skin (control), which was assigned a value of 100% and are expressed as the mean ± SD; $n = 13$. Significant increase versus control skin, $^{*}P < 0.001$.

targeting could be achieved through the use of novel demethylating agents or inhibitors of histone deacetylation, which would correct aberrant DNA hypermethylation patterns in UV-exposed skin and restore normal growth control in skin cells.

Funding

National Institutes of Health (CA140832 to S.K.K.); Veterans Administration Merit Review Award (S.K.K.)

Conflict of Interest Statement: None declared.

References

1. Ehrlich,M. (2000) DNA methylation in cancer: too much, but also too little. *Oncogene*, **21**, 5400–5413.
2. Jones,P.A. *et al*. (1999) Cancer epigenetics comes of age. *Nat. Genet.*, **21**, 163–167.
3. Zingg,J.M. *et al*. (1997) Genetic and epigenetic aspects of DNA methylation on genome expression, evolution, mutation and carcinogenesis. *Carcinogenesis*, **18**, 869–882.
4. Jones,P.A. *et al*. (2002) The fundamental role of epigenetic events in cancer. *Nat. Rev. Genet.*, **3**, 415–428.
5. Laird,P.W. *et al*. (1996) The role of DNA methylation in cancer genetic and epigenetics. *Annu. Rev. Genet.*, **30**, 441–464.
6. Baylin,S.B. (2000) DNA hypermethylation in tumorigenesis: epigenetics joins genetics. *Trends Genet.*, **16**, 168–174.
7. Jones,P.A. (2002) DNA methylation and cancer. *Oncogene*, **21**, 5358–5360.
8. Bird,A.P. (1986) CpG-rich islands and the function of DNA methylation. *Nature*, **321**, 209–213.
9. Antequera,F. *et al*. (1993) CpG islands. *EXS*, **64**, 169–185.
10. Robertson,K.D. (2005) DNA methylation and human disease. *Nat. Rev.Genet.*, **6**, 597–610.
11. Goodman,J.I. *et al*. (2002) Altered DNA methylation: a secondary mechanism involved in carcinogenesis. *Annu. Rev. Pharmacol. Toxicol.*, **42**, 501–525.
12. Counts,J.L. *et al*. (1995) Alterations in DNA methylation may play a variety of roles in carcinogenesis. *Cell*, **83**, 13–15.
13. Chen,W.Y. *et al*. (2003) Heterozygous disruption of Hic1 predisposes mice to a gender-dependent spectrum of malignant tumors. *Nat. Genet.*, **33**, 197–202.
14. Tommasi,S. *et al*. (2005) Tumor susceptibility of Rassf1a knockout mice. *Cancer Res.*, **65**, 92–98.
15. Herman,J.G. *et al*. (2003) Gene silencing in cancer in association with promoter hypermethylation. *N. Engl. J. Med.*, **349**, 2042–2054.
16. Wade,P.A. (2001) Methyl CpG-binding proteins and transcriptional repression. *Bioessays*, **23**, 1131–1137.
17. Bird,A.P. *et al*. (1999) Methylation-induced repression-belts, braces, and chromatin. *Cell*, **99**, 451–454.
18. Ng,H.H. *et al*. (2000) Active repression of methylated genes by the chromosomal protein MBD1. *Mol. Cell. Biol.*, **20**, 1394–1406.
19. Okano,M. *et al*. (1999) DNA methyltransferases Dnmt3a and Dnmt3b are essential for de novo methylation and mammalian development. *Cell*, **99**, 247–257.
20. Xie,S. *et al*. (1999) Cloning, expression and chromosome locations of the human DNMT3 gene family. *Gene*, **236**, 87–95.
21. Bachman,K.E. *et al*. (2001) Dnmt3a and Dnmt3b are transcriptional repressors that exhibit unique localization properties to heterochromatin. *J. Biol. Chem.*, **276**, 32282–32287.
22. Fuks,F. *et al*. (2001) Dnmt3a binds deacetylases and is recruited by a sequence specific repressor to silence transcription. *EMBO J.*, **20**, 2536–2544.
23. Mukhtar,H. *et al*. (1996) Photocarcinogenesis: mechanisms, models and human health implications. *Photochem. Photobiol.*, **63**, 355–447.
24. Issa,J.P. *et al*. (2001) Accelerated age-related CpG island methylation in ulcerative colitis. *Cancer Res.*, **61**, 3573–3577.
25. Sathyanarayana,U.G. *et al*. (2007) Sun exposure related methylation in malignant and non-malignant skin lesions. *Cancer Lett.*, **245**, 112–120.
26. Meeran,S.M. *et al*. (2009) Inhibition of UVB-induced skin tumor development by drinking green tea polyphenols is mediated through DNA repair and subsequent inhibition of inflammation. *J. Invest. Dermatol.*, **129**, 1258–1270.
27. Mantena,S.K. *et al*. (2005) Orally administered green tea polyphenols prevent ultraviolet radiation-induced skin cancer in mice through activation of cytotoxic T cells and inhibition of angiogenesis in tumors. *J. Nutr.*, **135**, 2871–2877.
28. Meeran,S.M. *et al*. (2007) Interleukin-12-deficiency is permissive for angiogenesis in UV radiation-induced skin tumors. *Cancer Res.*, **67**, 3785–3793.
29. Sharma,S.D. *et al*. (2007) Dietary grape seed proanthocyanidins inhibit UVB-induced oxidative stress and activation of mitogen-activated protein

kinases and nuclear factor-κB signaling in *in vivo* SKH-1 hairless mice. *Mol. Cancer Ther.*, **6**, 995–1005.
30. Cui,X. *et al*. (2006) Chronic oral exposure to inorganic arsenate interferes with methylation status of p16INK4a and RASSF1A and induces lung cancer in A/J mice. *Toxicol. Sci.*, **91**, 372–381.
31. Bardeesy,N. *et al*. (2002) Obligate roles for p16Ink4a and p19Arf-p53 in the suppression of murine pancreatic neoplasia. *Mol. Cell Biol.*, **22**, 635–643.
32. Magdinier,F. *et al*. (2001) Selective association of the methyl-CpG binding protein MBD2 with the silent p14/p16 locus in human neoplasia. *Proc. Natl Acad. Sci. USA*, **98**, 4990–4995.
33. Gonzalgo,M.L. *et al*. (1998) The role of DNA methylation in expression of the p19/p16 locus in human bladder cancer cell lines. *Cancer Res.*, **58**, 1245–1252.
34. Hoon,D.S. *et al*. (2004) Profiling epigenetic inactivation of tumor suppressor genes in tumors and plasma from cutaneous melanoma patients. *Oncogene*, **23**, 4014–4022.
35. Allen,N.P. *et al*. (2007) RASSF6 is a novel member of the RASSF family of tumor suppressors. *Oncogene*, **26**, 6203–6211.
36. Mori,T. *et al*. (2005) Predictive utility of circulating methylated DNA in serum of melanoma patients receiving biochemotherapy. *J. Clin. Oncol.*, **23**, 9351–9358.
37. El-Osta,A. *et al*. (2002) Precipitous release of methyl-CpG binding protein 2 and histone deacetylase 1 from the methylated human multidrug resistance gene (MDR1) on activation. *Mol. Cell. Biol.*, **22**, 1844–1857.
38. Cross,S.H. *et al*. (1997) A component of the transcriptional repressor MeCP1 shares a motif with DNA methyltransferase and HRX proteins. *Nat. Genet.*, **16**, 256–259.
39. Mittal,A. *et al*. (2003) Exceptionally high protection of photocarcinogenesis by topical application of (-)-epigallocatechin-3-gallate in hydrophilic cream in SKH-1 hairless mouse model: relationship to inhibition of UVB-induced global DNA hypomethylation. *Neoplasia*, **5**, 555–565.
40. Melnikova,V.O. *et al*. (2005) Cellular and molecular events leading to the development of skin cancer. *Mutat. Res.*, **571**, 91–106.
41. Matsumura,Y. *et al*. (2004) Toxic effects of ultraviolet radiation on the skin. *Toxicol. Appl. Pharmacol.*, **195**, 298–308.
42. Tommasi,S. *et al*. (1997) Sunlight induces pyrimidine dimers preferentially at 5-methylcytosine bases. *Cancer Res.*, **57**, 4727–4730.
43. Jonason,A.S. *et al*. (1996) Frequent clones of p53-mutated keratinocytes in normal human skin. *Proc. Natl Acad. Sci. USA*, **93**, 14025–14029.
44. Grönniger,E. *et al*. (2010) Aging and chronic sun exposure cause distinct epigenetic changes in human skin. *PLoS Genet.*, **6**, e1000971.
45. Boyes,J. *et al*. (1991) DNA methylation inhibits transcription indirectly via a methyl-CpG binding protein. *Cell*, **64**, 1123–1134.
46. Baylin,S.B. (2005) DNA methylation and gene silencing in cancer. *Nat. Clin. Pract. Oncol.*, **2**, 4–11.
47. Fried,L. *et al*. (2008) The reactive oxygen-driven tumor: relevance to melanoma. *Pigment Cell Melanoma Res.*, **21**, 117–122.
48. Arbiser,J.L. *et al*. (2004) Involvement of p53 and p16 tumor suppressor genes in recessive dystrophic epidermolysis bullosa-associated squamous cell carcinoma. *J. Invest. Dermatol.*, **123**, 788–790.

Received November 6, 2010; revised December 13, 2010;
accepted December 20, 2010